First performance results of the Phobos silicon detectors

H. Pernegger[4] ⋆ , B.B.Back[1], M.D.Baker[2], D.S.Barton[2], R.R.Betts[1,6], R.Bindel[7], A.Budzanowski[3], W.Busza[4], A.Carroll[2], M.P.Decowski[4], E.Garcia[7], N.George[1], K.Gulbrandsen[4], S.Gushue[2], C.Halliwell[6], J.Hamblen[8], G.A.Heintzelman[2], C.Henderson[4], R.Hołyński[3], D.J.Hofman[6], B.Holzman[6], E.Johnson[8], J.L.Kane[4], J.Katzy[4,6], N. Khan[8], W.Kucewicz[6,9], P.Kulinich[4], W.T.Lin[5], S.Manly[8,], D.McLeod[6], J.Michałowski[3], A.Mignerey[7], J.Mülmenstädt[4],R.Nouicer[6], A.Olszewski[2,3], R.Pak[2], I.C.Park[8], C.Reed[4], L.P.Remsberg[2], M.Reuter[6], C.Roland[4], G.Roland[4], L.Rosenberg[4], P.Sarin[4], P.Sawicki[3], W.Skulski[8], S.G.Steadman[4], G.S.F.Stephans[4], P.Steinberg[2], M.Stodulski[3], A.Sukhanov[2], J.-L.Tang[5], R.Teng[8], A.Trzupek[3], C.Vale[4], G.J.van Nieuwenhuizen[4], R.Verdier[4], B.Wadsworth[4], F.L.H.Wolfs[8], B.Wosiek[3], K.Woźniak[3], A.H.Wuosmaa[1], B.Wysłouch[4],

[1] Physics Division, Argonne National Laboratory, Argonne, IL 60439-4843

[2] Chemistry and Collider-Accelerator Departments, Brookhaven National Laboratory, Upton, NY 11973-5000

[3] Institute of Nuclear Physics, Kraków, Poland

[4] Laboratory for Nuclear Science, Massachusetts Institute of Technology, Cambridge, MA 02139-4307

[5] Department of Physics, National Central University, Chung-Li, Taiwan

[6] Department of Physics, University of Illinois at Chicago, Chicago, IL 60607-7059

[7] Department of Chemistry, University of Maryland, College Park, MD 20742

[8] Department of Physics and Astronomy, University of Rochester, Rochester, NY 14627

[9] University of Mining and Metallurgy, Kraków, Poland

Abstract

The Phobos experiment concluded its first year of operation at RHIC taking data in Au-Au nucleus collisions at $\sqrt{s_{nn}}$=65GeV and 130 GeV/nucleon pair. First preliminary results of the performances of our silicon detectors in the experiment are summarized. The Phobos experiment uses silicon pad detectors for tracking and multiplicity measurements, which vary strongly in their pad geometry. In this paper we compare the signal response, the signal uniformity and signal-to-noise performance as measured in the experiment for the different geometries. Additionally we investigate effects of very high channel occupancy on the signal response.

keywords: silicon pad detector, RHIC, heavy ion collision, silicon signal

---

⋆ present address: CERN Div. EP, CH-1211 Geneve 23, Switzerland, `heinz.pernegger@cern.ch`

Preprint submitted to Elsevier Preprint *23 January 2001*

1 Introduction

The Phobos experiment at the Relativistic Heavy Ion Collider (RHIC) studies hadronic matter at very high energy density, which are produced in Au-Au collisions to search for signatures of quark-gluon plasma. The experimental setup of the experiment is largely based on silicon pad detectors, which are used in two complementary detector parts. A single layer, large coverage silicon multiplicity detector measures the number of charge particles produced in the collision over in a large pseudo-rapidity range. The other detector part comprises two silicon spectrometer arms, which consist of 16 layers of silicon detectors. The spectrometer arms track and identify charged particles in a 2T magnetic field. The layout of the experiment and its detector parts is illustrated in figure 1. Details of the experiment layout can be found in references [1] and [2].

Both detector systems are based on single-sided, AC coupled, double metal silicon pad detectors with pad sizes varying from 1 to 30mm^2. The larger pads are used in the multiplicity detector to achieve hermetic coverage with a limited number of channels (25000), while the spectrometer uses detectors with smaller pads, a total of 120 000 for both arms, for track reconstruction. Table 1 summarizes the different pad geometries used. A detailed description of the silicon detectors used can be found in reference [3]. All detector pads are readout via trace lines in a second metal layer on the wafer p-side, which connect to VAHDR1 front-end readout chips [4] [5]. The VAHDR1 readout chip provides an analog measurement of the ionization charge deposited in the silicon detector for each pad. The analog signals are digitized by 12-bit ADCs in the readout system. The readout electronics also incorporates a channel per channel gain calibration, which is based on injection of a controlled amount of charge into the preamplifier. This allows us to relate the measured ADC information to the primary ionization signal. Details of the calibration system can be found in reference [6].

2 Signal response of the multiplicity detector

The multiplicity detector measures the charged particle multiplicity using the particle's ionization in a single layer of silicon. In order to extract final numbers for the multiplicity versus pseudo-rapidity and azimuthal angle, a precise knowledge of the detector response and a careful calibration is essential.

As part of the performance evaluation and physics analysis of this detector part we studied the effect of high occupancy on the response, the uniformity of the signal amplitude for different wafer layouts and the response uniformity within each wafer type.

With a measured charged particle multiplicity in Au-Au collisions [7] of 550 particles per unit of pseudo-rapidity for central Au-Au collisions, the central parts of the octagon multiplicity detectors have to cope with channel occupancies exceeding 80%. We found a shift of the chip's signal baseline depending on the total input charge into the chip. Figure 3 shows the chip baseline, which is determined from the analog information of channels without hits, versus the total integrated signal deposited on the chip. The figure illustrates that baseline shifts up to and beyond 100keV can be fully corrected using the information of channels without hits.

After the hit signals are corrected for baseline shifts, electronic gain, track inclination and detector thickness, we measured the single hit signal distribution for events and detector areas with different hit occupancy. The signals are normalized to a 300μm long path in silicon. Figure 2b-d shows the signal distribution for four selections: detectors with channel occupancy of 0 to 10%, 10% to 20%, 20 to 50% and greater than 80%. We found a 6% decrease in the most probable signal for detectors with high occupancy with respect to detectors with low occupancy.

The uniformity of the signal response across the multiplicity detector is important for the estimation of the charged particle multiplicity through their integrated charge deposition. Figure 4 shows the calibrated signal distribution, corrected for track angle and detector thickness, for the octagon and ring multiplicity detectors. We measure a most probable signal of 93keV and 85keV for octagon and ring detectors respectively. The solid line in figure 4 shows the fit, which is used to determine the most probable signal. Slight differences in the peak signal from ring and octagon detector may be due to their different acceptance in the momentum space of the produced particle, where the octagon detectors sample more low momentum particles than the ring detectors. The insert in each figure show the relative variation of the most probable signal within the octagon and ring sensors. The most probable signal in each pad row is plotted versus pad row number, which would reveal non-uniformities caused by the parasitic capacitance of readout lines on top of the pads. The uniformity within the sensors is better than $\pm 3\%$ for the octagon and $\pm 1\%$ for the ring detector.

3 Signal response of the silicon spectrometer and vertex detector

The silicon detectors of the spectrometer have finer granularity than the multiplicity detector to allow acurate tracking of each charged particle in its acceptance. The first 6 planes of each arm are in a region without magnetic field, while the remaining planes are located in a 2T magnetic field to determine the particle momentum. Particle identification for pions, kaons and proton is possible through multiple dE/dx measurements in several silicon planes traversed by the particle..

To achieve good separation of pion-, kaon-, and proton-dE/dx bands it is essential that the signal response, after gain, track angle and detector thickness correction, is uniform through out the spectrometer and only depends on particle type and momentum. Given the fact that the wafer layout strongly varies in the spectrometer, we measured the signal response for the different layout geometries. The variation in pad size and readout line length leads to different internal capacitive networks, which may influence channel to channel crosstalk or signal loss due to parasitic capacitances [8].

The data used for this performance check where obtained with the magnetic field off, to allow straight line tracking through the entire spectrometer. The signals of each pad where corrected for their channel gain, track angle and detector thickness. Figure 5 shows the signal distributions for vertex and spectrometer wafer layouts, where IV and OV wafers have a rather "strip-like" configuration, T1 and T2 wafers have small pads and T3, T4 and T5 have larger pads (see table 1 for detailed dimensions). The signal distrbutions correspond to 300μm path in silicon. The fit of a convoluted landau and gauss function to the distributions, which is shown in the plot as solid line, yield a very uniform most probable landau signal 85 keV for vertex and spectrometer with exception of the detector types mounted closest to the interaction point (inner vertex and T1 wafers), which show slightly higher signals. The higher signal on the closest detectors may be due to their larger acceptance to low momentum particles. We also tested the relative variation of the signal within each wafer type, which is displayed in figure 6. Typical pad-to-pad variations of the signal within each wafer are only $\pm 1\%$.

4 Signal-to-noise performance

Differences in the pad geometry will result in differences in pad leakage currents and load capacitance on the amplifier input. As a consequence we expect the noise to be larger for detectors with large pads and long readout lines.

We determined the most probable signal and equivalent noise charge (ENC) from data recorded during the physics run. Figure 7 shows the most probable landau signal (a), which was extracted from a fit to the signal distribution, and equivalent noise charge (b), which was determined from the raw channel noise and corrected for common mode noise on a chip-per-chip basis. On detectors types mounted closest to the interaction point (T1, Oct, IV) we observe a 6%

higher signal than on detector types mounted further away from the interaction region (T2,T3,T4,T5, Rng). Although the detector types further away from the interaction region vary strongly in their pad and readout geometries, they yield a very uniform signal response. The measured noise shows clearly the dependence on the pad size and readout line geometry, with an ENC of 1100 to 1300e- for detector types with small pads. The two detector types with large pads, octagon and ring, show the expected higher noise. The values measured during the physics run are in good agreement with calculations and laboratory measurements during the assembly of the detector modules [3].

5 Summary

The Phobos experiment uses a wide range of silicon pad detectors for tracking, particle identification and charged particle multiplicity measurements. In all these measurements the actual signal response of the detector plays a crucial role. Based on a data set recorded during the first physics run at RHIC we analysed the signal response for the different detector geometries and compared signal amplitude, uniformity and signal-to-noise performance. Although the detector types vary strongly in pad size and readout geometry we found only a small variation in the most probable signal. The average pad-to-pad signal uniformity is excellent for our application with a variation of less than $\pm 2\%$ typically. The high multiplicity of central Au-Au collisions result in very high channel occupancies, which can exceed 80%. We observed parasitic effects at very high occupancies like baseline shifts of the electronics and gain changes, which can be corrected in the offline analysis. The signal-to-noise performance exceeds 15:1 on all detector types for our choice of readout electronics, which is significantly better than our design requirement of 10:1.

References

[1] B. Back et al., "Phobos Conceptual Design Report", BNL 1994.

[2] J.M. Katzy et al., Nuclear Physics A 611(1999)690

[3] B. Back et al., Nucl. Inst. and Meth. A 447(2000)257-263

[4] E. Nygard et al., Nucl. Inst. and Meth. A 301(1991)506-516

[5] VAHDR1 chip produced in AMS 1.2μm process by IDE AS, Veritasveien9, N-1323 Hovik, Norway

[6] E. Giesmayer et al., "Calibration system for the Phobos silicon detector system", submitted for publication to IEEE, Trans. Nucl. Science.

[7] PHOBOS collaboration, B. Back et al., Phys. Rev. Lett. 85, 3100 (2000)

[8] H. Pernegger, Nucl. Inst. and Meth. A 419 (1998) 549-555

Sensor type	Pad size (width ×height mm^2)	Pad rows× columns
Spectrometer		
Type 1 (T1)	1×1	22×70
Type 2 (T2)	0.43×6	8×64
Type 3 (T3)	0.67×7.5	8×64
Type 4 (T4)	0.67×15	4×64
Type 5 (T5)	0.67×19	4×64
Multiplicity		
Octagon (Oct)	2.6×9.5	30×4
Ring (Rng)	≈ 50	64 $r\phi$ pads
Inner vertex (IV)	0.32×23.3	2×256
Outer vertex (OV)	0.32×46.6	1×256

Table 1
Pad size and number of pads per detector for the different layouts used the PHOBOS silicon detectors

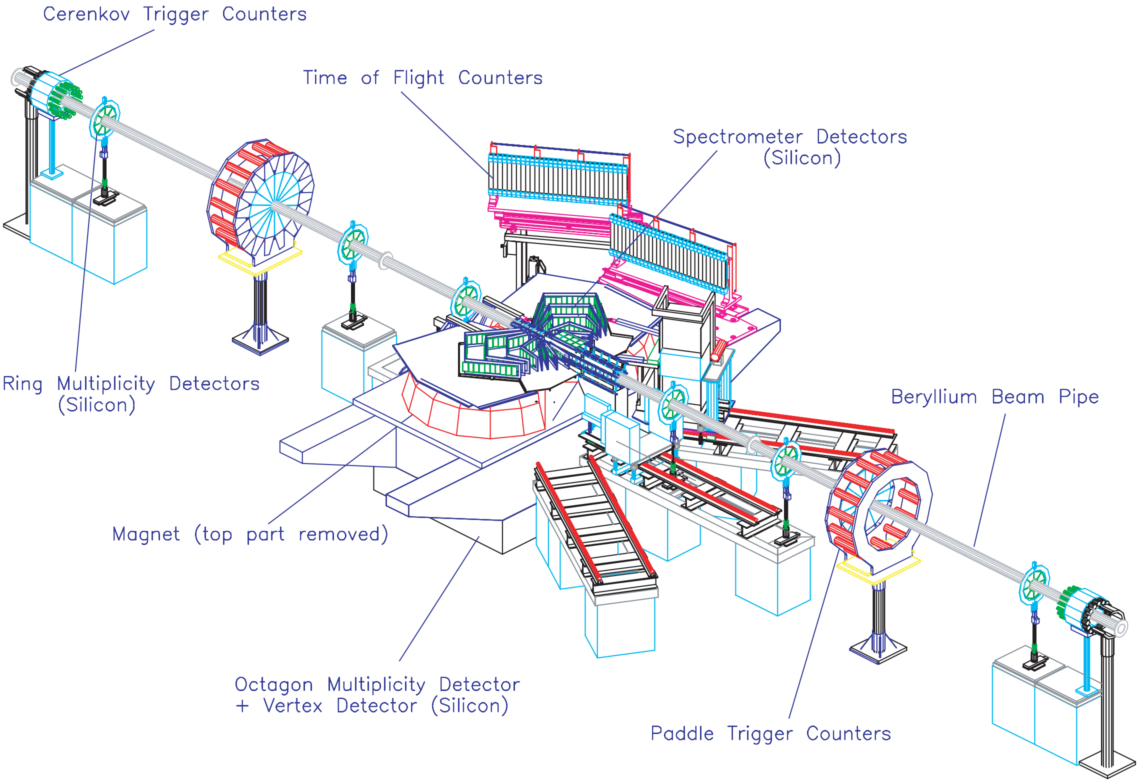

Fig. 1. Schematic layout of the Phobos experiment

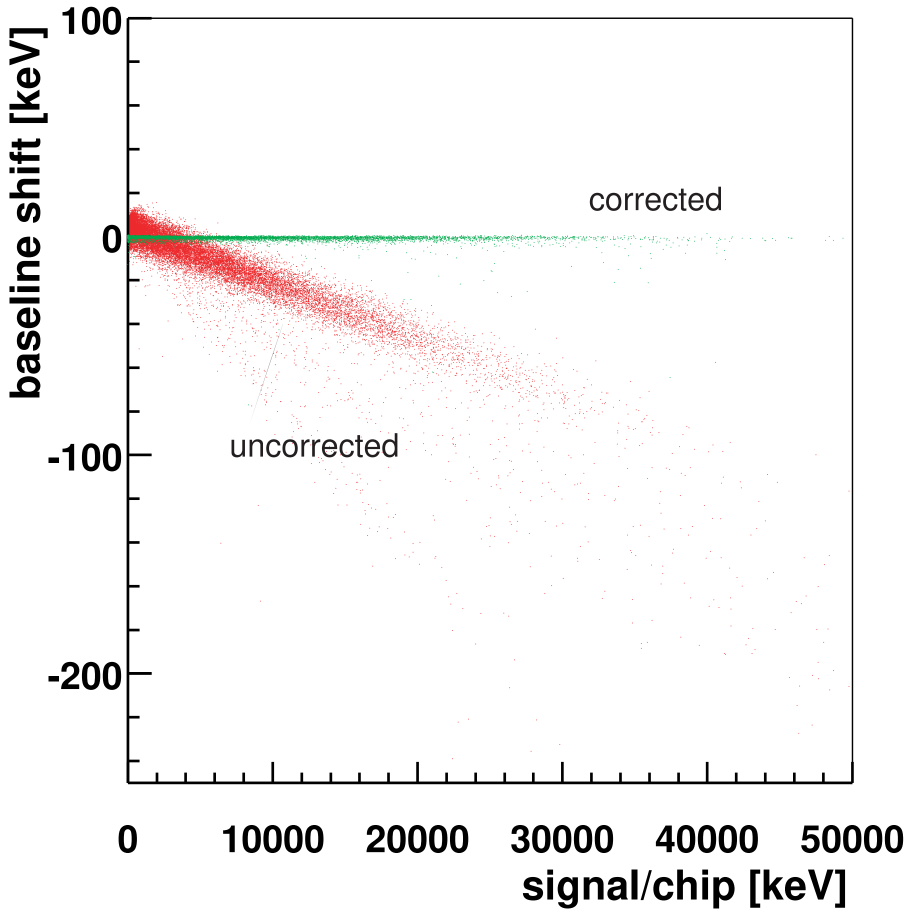

Fig. 2. Chip baseline shift versus total chip input signal before and after offline correction

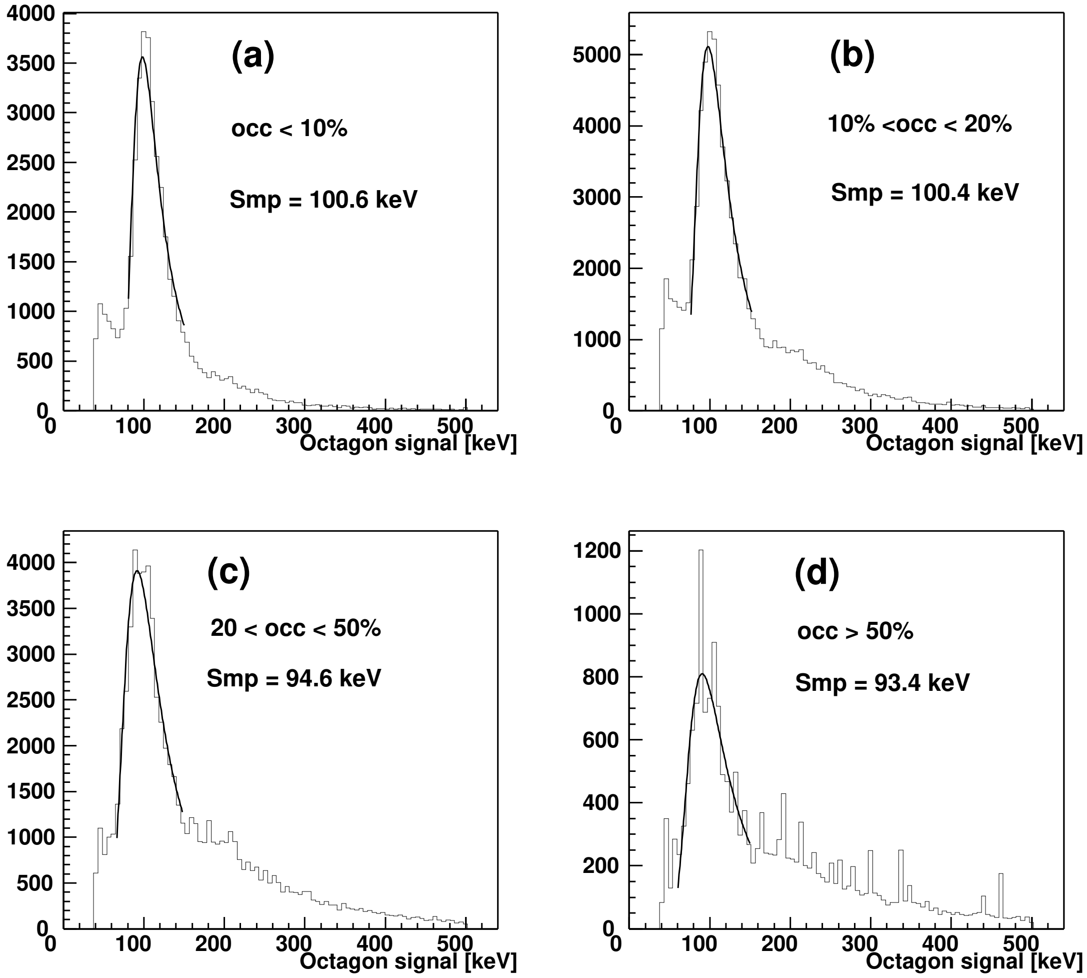

Fig. 3. Signal distributions for four different selections of channel occupancy per detector (plot a to d), defined as number of channels with a hit over total number of channel per detector

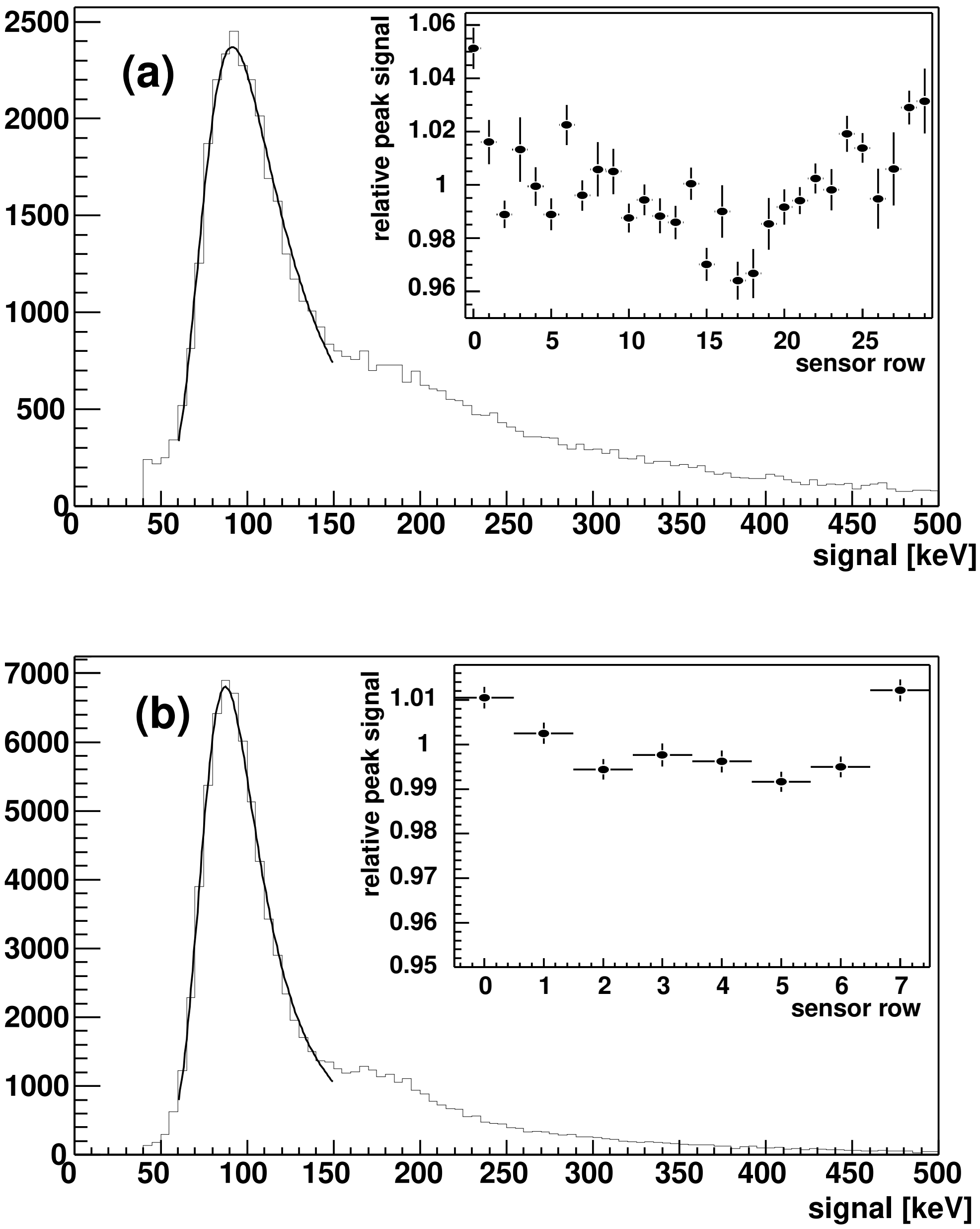

Fig. 4. Calibrated signal distributions and relative signal uniformity (insert) as measured on the multiplicity octagon (a) and ring (b) detectors.

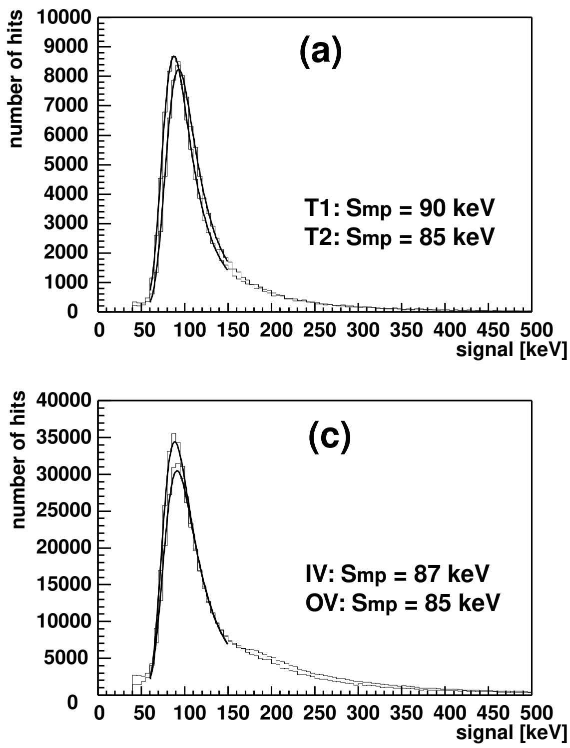

Fig. 5. Calibrated signal distributions measured on the tracking spectrometer and vertex detectors.

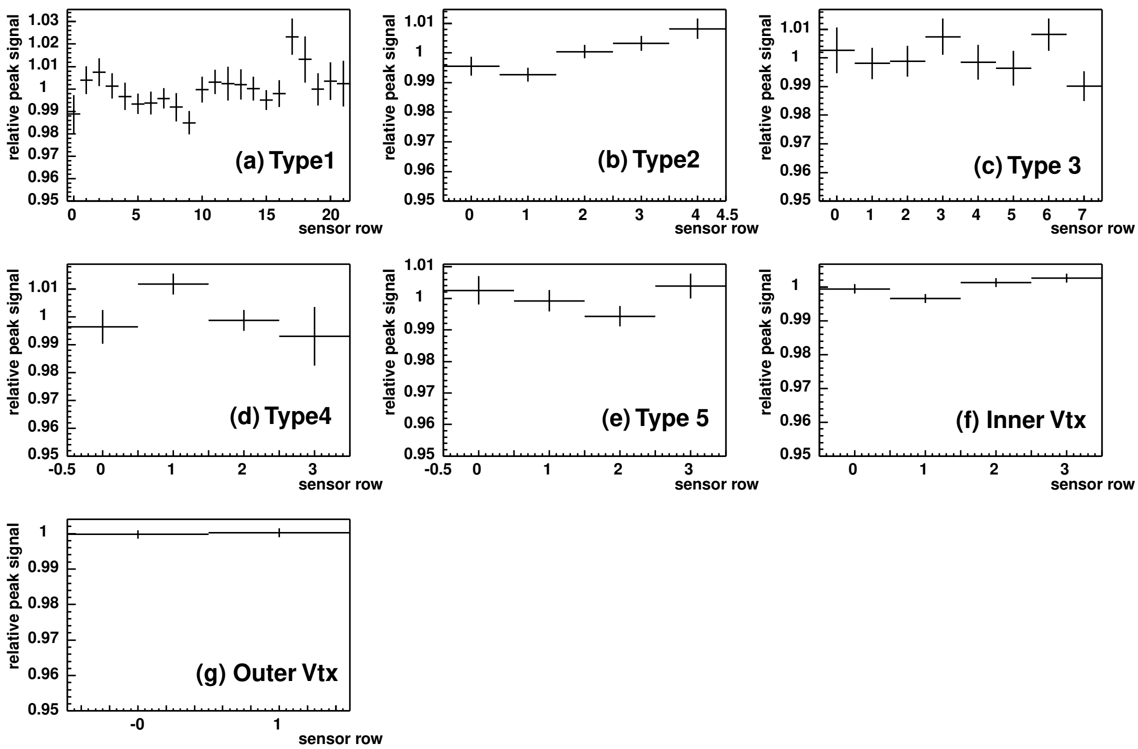

Fig. 6. Relative signal uniformity on the tracking spectrometer and vertex detectors.

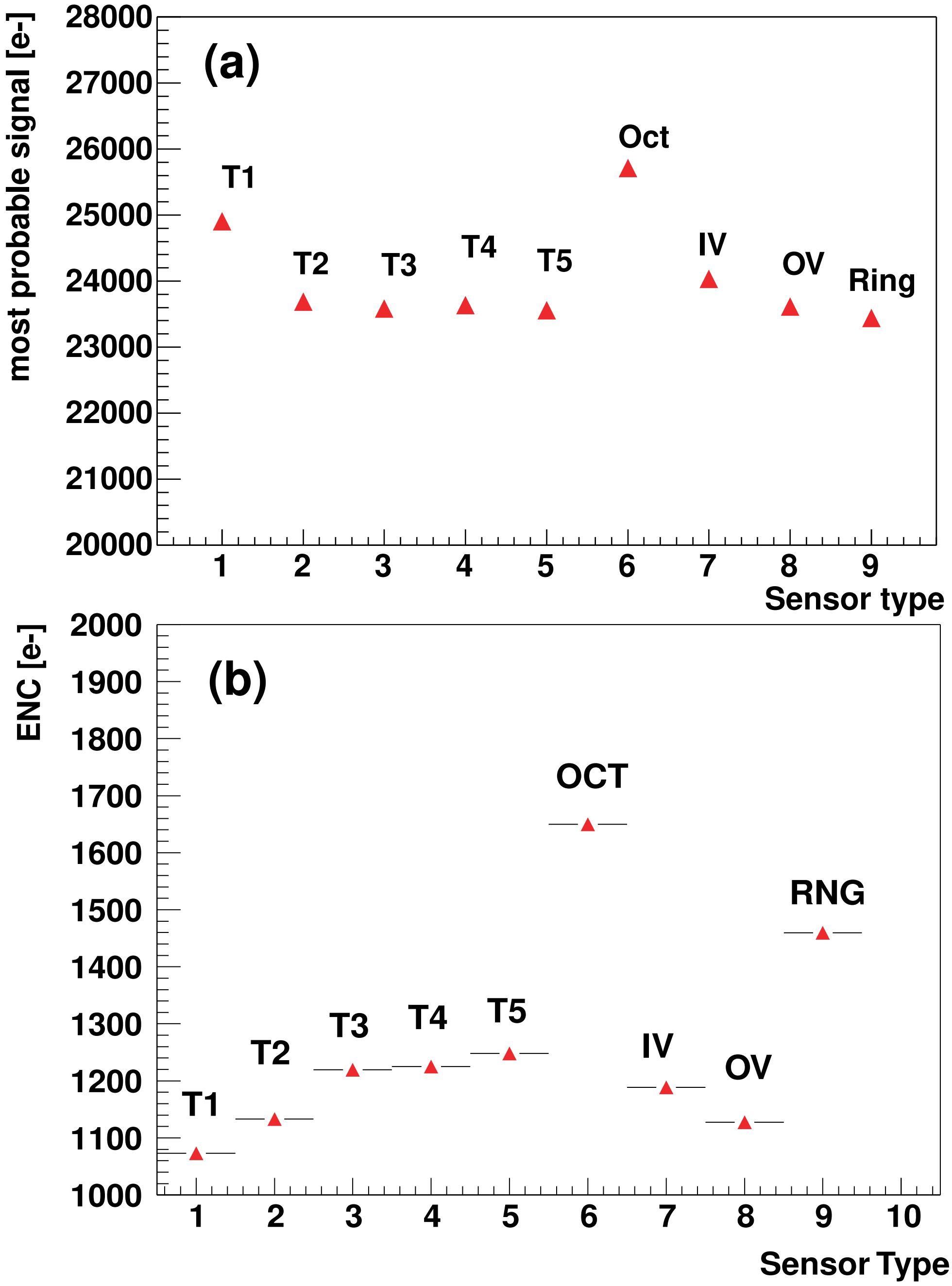

Fig. 7. Most probable calibrated signal (a) and equivalent noise charge (b) for different detector layouts.